

Comparing immunogenicity and protective efficacy of the yellow fever 17D vaccine in mice

Ji Ma ^a, Robbert Boudewijns ^a, Lorena Sanchez-Felipe ^a, Niraj Mishra ^{a,*}, Thomas Vercruysse ^{a,b},
Dieudonné Buh Kum ^{a,†}, Hendrik Jan Thibaut ^{a,b}, Johan Neyts ^{a,c} and Kai Dallmeier ^{a,c}

^aKU Leuven Department of Microbiology, Immunology and Transplantation, Laboratory of Virology, Molecular Vaccinology and Vaccine Discovery, Rega Institute, Leuven, Belgium; ^bKU Leuven Department of Microbiology, Immunology and Transplantation, Laboratory of Virology and Chemotherapy, Translational Platform Virology and Chemotherapy, Rega Institute, Leuven, Belgium; ^cGlobal Virus Network (GVN), Baltimore, MD, USA

ABSTRACT

The live-attenuated yellow fever 17D (YF17D) vaccine is one of the most efficacious human vaccines and also employed as a vector for novel vaccines. However, in the lack of appropriate immunocompetent small animal models, mechanistic insight in YF17D-induced protective immunity remains limited. To better understand YF17D vaccination and to identify a suitable mouse model, we evaluated the immunogenicity and protective efficacy of YF17D in five complementary mouse models, i.e. wild-type (WT) BALB/c, C57BL/6, IFN- α/β receptor (*IFNAR*^{-/-}) deficient mice, and in WT mice in which type I IFN signalling was temporally ablated by an IFNAR blocking (MAR-1) antibody. Alike in *IFNAR*^{-/-} mice, YF17D induced in either WT mice strong humoral immune responses dominated by IgG2a/c isotype (Th1 type) antibodies, yet only when IFNAR was blocked. Vigorous cellular immunity characterized by CD4⁺ T-cells producing IFN- γ and TNF- α were mounted in MAR-1 treated C57BL/6 and in *IFNAR*^{-/-} mice. Surprisingly, vaccine-induced protection was largely mouse model dependent. Full protection against lethal intracranial challenge and a massive reduction of virus loads was conferred already by a minimal dose of 2 PFU YF17D in BALB/c and *IFNAR*^{-/-} mice, but not in C57BL/6 mice. Correlation analysis of infection outcome with pre-challenge immunological markers indicates that YFV-specific IgG might suffice for protection, even in the absence of detectable levels of neutralizing antibodies. Finally, we propose that, in addition to *IFNAR*^{-/-} mice, C57BL/6 mice with temporally blocked IFN- α/β receptors represent a promising immunocompetent mouse model for the study of YF17D-induced immunity and evaluation of YF17D-derived vaccines.

ARTICLE HISTORY Received 6 August 2021; Revised 29 October 2021; Accepted 16 November 2021

KEYWORDS Yellow fever 17D; mouse models; correlate of protection; type I IFN response; live-attenuated vaccine

Introduction

Yellow fever virus (YFV) is a mosquito-borne positive sense RNA virus of the genus *Flavivirus*, family *Flaviviridae* [1]. YFV is mainly endemic in Africa and tropical regions of South America, causing approximately 200,000 infections and 30,000 mortalities annually by estimation [2]. No specific antiviral therapy is available and YFV outbreaks are mainly contained by the deployment of a live-attenuated YF17D vaccine developed in the 1930s by Max Theiler and colleagues [3]. With more than 800 million doses having been administered globally and only a handful of complications reported, YF17D has proved itself one of the most efficacious and safe human vaccines ever developed and is therefore considered as a benchmark for a successful vaccine [4]. A single dose of YF17D vaccination induces in vaccinees (i) almost 100% seroconversion by 10 days post-vaccination, (ii) high YFV-specific neutralizing antibody


(nAbs) titers as well as (iii) robust, long-lived, polyfunctional memory T cell responses, possibly providing life-long protection against all known WT YFV strains [5–7]. In addition, the YF17D vaccine is also used as a viral vector for the development of novel vaccines. Two YF17D-based vaccines against JEV (Imojev[®]) and DENV (Dengvaxia[®]) got market authorization for human use [8]. Furthermore, several promising YF17D-vectored vaccine candidates are currently in development [9–11]. Due to its excellent efficacy and favourable safety profile, YF17D offers thus a unique vaccine model to study human immune responses to vaccination which in turn may contribute to the development of novel and better vaccines [12,13].

Models for experimental study of YF17D vaccination are limited. As humans are practically inapplicable, non-human primate models are prohibitively expensive and hamsters require adapted virus for infection, mouse models represent the most practical

CONTACT Kai Dallmeier  kai.dallmeier@kuleuven.be

*Current affiliation: Department of Cell and Gene Therapy, Biopharma Division, Intas Pharmaceuticals, Ahmedabad, India

†Current affiliation: Aligos Belgium, Leuven, Belgium.

 Supplemental data for this article can be accessed at <https://doi.org/10.1080/22221751.2021.2008772>

© 2021 The Author(s). Published by Informa UK Limited, trading as Taylor & Francis Group.

This is an Open Access article distributed under the terms of the Creative Commons Attribution-NonCommercial License (<http://creativecommons.org/licenses/by-nc/4.0/>), which permits unrestricted non-commercial use, distribution, and reproduction in any medium, provided the original work is properly cited.

option [14]. Among those mouse models, BALB/c mice are frequently used for the analysis of humoral immunity in preclinical vaccine testing, whereas C57BL/6 mice are commonly used for mechanistic studies and for the assessment of vaccine-induced cellular immunity given the availability of different knockout substrains [15,16]. However, YF17D vaccine strains are severely attenuated in immunocompetent WT adult mice and need to be injected intracranially (i.c.) to establish productive infection, less relevant to natural infection and pathogenesis [17,18].

In contrast, mice deficient in type I interferon (IFN- α/β) signalling such as mice with a genetic ablation of IFN- α/β receptor (IFNAR) expression, namely A129 and *IFNAR*^{-/-} mice are highly susceptible to YF17D infection and are therefore widely used as surrogate model to study mechanisms underlying the pathogenesis of WT YFV, attenuation and immunogenicity of YF17D as well as YF17D-derived vaccines assessment [15,17,19,20]. However, in this model, YF17D replicates disproportionately as type I IFN responses normally controls virus replication and dissemination of YFV both in mice [21,22] as well as in human [23,24]. In addition, type I IFN plays an essential role in the early activation of B and T cell responses and in the enhancement of antigen presentation by dendritic cells [25–28]. As a consequence, defects in type I IFN responses may result in a diminished capacity to expand and generate optimal B cell and memory T cell responses after viral infections in mice [29–31]. Immune responses after YF17D vaccination in IFN- α/β receptors knockout mice are therefore generally considered imprecise and to provide only limited insight relevant into the human [32,33]. Thus, the establishment of an immunocompetent mouse model is key to fully explore the molecular mechanisms of YF17D-induced protective immunity.

To better understand YF17D-induced immunogenicity and to justify an immunocompetent mouse model for the study of YF17D and YF17D-derived vaccines, we compared YF17D-induced humoral and cellular responses in a set of complementary mouse models, including *IFNAR*^{-/-}, WT BALB/c and C57BL/6 and same WT mice in which type I IFN signalling was temporarily blocked [34]. Resulting protective efficacy of YF17D was evaluated by a stringent intracranial challenge. Last, comprehensive analysis was performed to quantitatively define correlates of protection between (i) immunological read-outs (humoral and cellular) and (ii) the level of protection parameters (survival and virus load) conferred by a wide range of YF17D doses.

Materials and methods

Cells and medium

Vero E6 (African green monkey) and BHK-21J (Baby hamster kidney fibroblasts) [35] cells were a generous

gift from Peter Bredenbeek, Leiden University, the Netherlands. Cells were maintained in seeding Medium (MEM Rega-3, Gibco, Belgium) supplemented with 10% fetal calf serum (FCS, Gibco, Belgium), 2 mM L-glutamine (Gibco, Belgium), 100 units/ml penicillin–streptomycin solution (Pen/Strep, Gibco, Belgium), 1% sodium bicarbonate (Gibco, Belgium), and incubated at 37°C, 5% CO₂. Virus culture and serum neutralization tests (SNT) were performed in assay medium (supplemented with 2% FCS).

Virus

YF17D strain, Stamaril® (Sanofi-Pasteur), was passaged three times in Vero E6 cells before use. Virus titers were determined by plaque assay on BHK-21J cells, expressed as plaque forming units, PFU/mL.

Mice

Six- to eight-week-old male and female *IFNAR*^{-/-} (C57BL/6 mice homozygous for an *IFNAR1* knockout mutation, B6.129S2-*Ifnar1*^{tm1Agt}) [36] (bred in-house), WT BALB/c and C57BL/6 mice (purchased from Janvier Labs, France) were used throughout this study. All experiments using mice strictly followed Belgian guidelines for animal experimentation and guidelines of the Federation of European Laboratory Animal Science Associations (FELASA). The Ethical Committee of the Animal Research Center of KU Leuven approved all experiments (project number P100/2019).

YF17D vaccination experiment in mice

For *in vivo* blocking studies, the anti-mouse *IFNAR1* monoclonal antibody (mAb) MAR1-5A3 (IgG1, Cat. no. I-401, Leinco Technologies, St. Louis, MO, USA), referred to as MAR1 was used, administered via the intraperitoneal (i.p.) route. As recommended for saturation of IFN- α/β receptors, WT mice received each a loading dose of 2 mg MAR1 one day prior to vaccination, followed by two more doses of each 0.5 mg at day 3 and 7 post-vaccination, respectively, considering a reported half-life of 5 days (Figure S5 (A)). MAb GIR-208 (Mouse IgG1, Cat. no. G737, Leinco Technologies) served as isotype control. All mice including non-treated WT mice and *IFNAR*^{-/-} mice were vaccinated i.p. with either 2 PFU or 2 × 10⁴ PFU virus at day 0, while sham group received the same volume of culture medium. The i.p. route was chosen for vaccination to ensure maximal exposure and a more consistent vaccination outcome in mice [10,11,17]. All mice were monitored daily for morbidity and mortality. Mice were bled weekly and serum was collected for indirect immunofluorescence assay (IIFA) and serum neutralization test

(SNT). Four weeks post-vaccination, mice were euthanized and spleens were harvested for ELISPOT and intracellular cytokine staining (ICS).

YFV-specific total IgG antibody detection by IIFA

Total YFV-specific IgG in mouse serum was determined as described [37], using a commercial Anti-YFV IgG IIFA kit (FI 2665-1010 G, EUROIMMUN, Germany) according to manufacturer's instructions, except for replacing secondary detection antibody and mounting medium by goat-anti-mouse IgG Alexa Fluor 488 (A11001, Life Technologies, 1:250 dilution) and 4',6-diamidino-2-phenylindole (DAPI; ProLong antifade reagent with DAPI; Thermo Fisher Scientific), respectively. IIFA was performed after 1/3 serial dilution of serum samples in dilution buffer and end point titers of each sample defined as the highest dilution that scored positive. Serum from non-vaccinated mice served as a negative control. Titers of > 1:30 for IgG were considered positive. Slides were visualized using a fluorescence microscope (FLoid Cell Imaging Station, Thermo Fisher Scientific).

YFV-specific IgG subtypes detection by IIFA

Titers of IgG subtypes were determined by a modified IIFA using an in-house developed fluorescence-based assay [10] and cells infected with a mCherry tagged variant of YF17D virus [11] as target antigen. In brief, BHK-21J cells grown in 96-well plates were infected with YF17D-mCherry virus at a multiplicity of infection (MOI) of 0.07 for 1 h at 37°C prior to incubation for 72 h at 37°C, then fixed with 4% paraformaldehyde and kept at 4°C until further use. Non-infected cells in adjacent columns of the same plate served as background controls. For the termination of end point titers, serial serum dilutions (1/3) were made on these IIFA plates on columns of infected cells and uninfected controls in parallel. Goat-anti-mouse IgG1, IgG2a, IgG2c (respectively 115-545-205, 115-545-206 and 115-545-208 from Jackson ImmunoResearch; all 1:250 diluted) were used as secondary antibody. After counterstaining with DAPI, fluorescence in the blue channel (cell nuclei, excitation at 405 nm), the green channel (binding antibodies, excitation at 480 nm) and red channel (control for virus infection, excitation at 570 nm) was measured on an ImmunoSpot® Series 6 Ultimate Reader and spots were counted using the ImmunoSpot® Series 6 Ultimate software (Cellular Technology Limited). For every serum dilution condition, the background signal of the uninfected control was subtracted from the signal of the infected cells. The IIFA end titer of each condition was

defined as the reciprocal of the highest dilution for which the background-corrected signal was positive and for which the ratio between the background-corrected signal of the previous dilution and this dilution was > 1.5.

YFV-specific neutralizing antibody detection by SNT

50% neutralizing antibody titers (SNT₅₀) were determined essentially as described, using a serum neutralization test (SNT) based on the inhibition of the virus-induced cytopathic effect (CPE) on BHK-21J cells [37]. In brief, sera were pre-incubated with each 100 TCID₅₀ of YF17D virus for 1 h at 37°C in serial dilutions 1:20, 1:66, 1:200, 1:660, 1:2000, and 1:6600 (in assay medium; each in triplicate), after which these serum/virus mixtures were added to BHK-21J grown in 96-well plates overnight (2 × 10⁴ cells/well in seeding medium) for further incubation at 37°C for 5 days. At day 5, medium was discarded and cells were stained with MTS/Phenazine methosulphate (PMS, Sigma-Aldrich) solution for 1 h at 37°C in the dark. Absorbance was measured at 498 nm using a microtiter plate reader (Safire, Tecan). CPE neutralization was calculated using the following formula: percent neutralization activity = percent CPE reduction = (OD_{Virus + Serum} - OD_{VC}) × 100 / (OD_{CC} - OD_{VC}), whereby OD is optical density; and 50% neutralization titers (SNT₅₀) were calculated using the Reed and Muench method [38]. Values from cells infected with 100 TCID₅₀ of YF17D without prior serum treatment served as positive virus control (VC), while uninfected cells served as negative cell control (CC). SNT₅₀ values for each sample represent geometric means of three independent repeats and data are presented as log₁₀ SNT₅₀. The assay has been validated against a standard plaque reduction neutralization assay (PRNT), yielding a strong correlation (Pearson correlation [R^2] = 0.71; P = 0.018) between log₁₀ YFV PRNT₅₀ and log₁₀ YFV SNT₅₀ titers in matched mouse serum samples [37].

YFV-specific T cell response analysis

Mouse spleen single-cell suspensions were prepared as described previously [10,37]. Vero E6 cells were infected with YF17D and cells subjected to serial freeze-thaw cycles four days post-infection, inactivated by 254 nm UV irradiation overnight and diluted cell lysate (50 µg/mL) was used as YF17D total antigen to serve as recall antigen. Non-infected Vero E6 cell lysate served as negative control. Likewise, MHC-I class-restricted YF17D NS3 peptide (ATLYRML) [39] (Eurogentec, Belgium) for H-2K^b C57BL/6 and *IFNAR*^{-/-} mice, MHC-I class-restricted YF17D envelope peptide (CYNAVLTHV) [40] (Eurogentec, Belgium) for H-2K^d BALB/c mice were used.

Intracellular cytokine staining (ICS) and flow cytometry

ICS was performed as described [10,11,37]. In brief, 2×10^6 mouse splenocytes per well were incubated overnight in IMDM medium (Gibco, Belgium) supplemented with 2% FCS and 2 mM L-glutamine with three different antigen conditions: (i) 50 µg/mL YF17D total antigen lysate, (ii) 50 µg/mL Vero E6 cell lysate, and (iii) 5 µg/mL MHC-I YF17D envelope peptide (for BALB/c), or 5 µg/mL MHC-I YF17D NS3 peptide (for C57BL/6 and *IFNAR*^{-/-}). After treatment with brefeldin A (Biolegend) for 4 h, cells were stained for viability with Zombie Aqua™ (Biolegend) for 15 min in the dark at room temperature. Subsequently, cells were strained with extracellular markers BV785™ anti-CD4 (GK1.5) and APC/Cy7 anti-CD8a (53-6.7), then fixed/permeabilized with Fixation/Permeabilization Solution (Fixation/Permeabilization Solution Kit, BD). Finally, cells were intracellularly stained with the following antibodies from Biolegend: APC anti-IFN-γ (XMG1.2), PE/Dazzle™ 594 anti-TNF-α (MP6-XT22), PerCP/Cyanine 5.5 anti-Granzyme B (GzmB, QA16A02). Samples were acquired on a BD LSRFortessa™ X-20 (BD). All data were normalized by subtraction of response in non-stimulated samples (incubated with non-infected Vero E6 cell lysates) from the response in corresponding stimulated samples. The gating strategy employed for ICS analysis is depicted in Figure S4. All flow cytometry data were analysed using FlowJo Version 10.6.1 (LLC).

ELISPOT

ELISPOT assays for the detection of IFN-γ-producing mouse splenocytes were performed with mouse IFN-γ kit (CTL Europe GmbH, Germany). Briefly, 6×10^5 fresh mouse splenocytes per well were incubated with the same concentration of antigen as described for ICS. After 48 h of incubation at 37°C, IFN-γ spots were visualized by stepwise addition of a biotinylated detection antibody, a streptavidin-enzyme conjugate and the substrate. Spots were counted using an ImmunoSpot S6 Universal Reader (CTL Europe GmbH) and normalized by subtracting the number of spots from samples incubated with non-infected Vero E6 cell lysates from those of stimulated samples.

YF17D vaccination and challenge experiment

MAR1 antibody was administered to WT mice according to the scheme shown in Figure S5A. All mice including MAR1-treated/non-treated WT mice and *IFNAR*^{-/-} mice were vaccinated i.p. with 2 PFU, 20 PFU, 2×10^3 PFU, or 2×10^4 PFU of

YF17D at day 0, while the sham-vaccinated group received culture medium. Mice were bled at day 21 post-vaccination before intracranial (i.c.) injection with 30 µL of 10^3 PFU of YF17D while deeply anaesthetized by using an anaesthetic combination of 0.4 µL atropine, 0.4 µL ketamine and 0.8 µL xylazine per gram body weight.

Likewise, to evaluate the protective efficacy of inactivated YF17D virus in mice, *IFNAR*^{-/-} mice were immunized with 2×10^4 PFU of either live or an equivalent amount of UV-inactivated YF17D (complete virus inactivation was confirmed by plaque assay and cytopathic effect assay) and then challenged. Serum samples from those mice were collected at days 7 and 21 post-vaccination.

All mice were monitored daily for signs of disease and weight change for 4 weeks. Sick mice were euthanized based on morbidity (hind limb paralysis, weakness, and ruffled fur) or weight loss of more than 25%. Mice that died within 4 days post-challenge (likely due to trauma from i.c. inoculation) were excluded from further survival analysis. Blood and brains were collected at euthanasia after challenge.

Quantification of viral loads in mouse brains by RT-qPCR

Total RNA was extracted from homogenized mouse brains using the NucleoSpin RNA virus 250 kit (Macherey Nagel, Belgium) according to the manufacturer's protocol. Viral RNA copies in brains were determined by RT-qPCR using a forward primer (5'-CAC GGC ATG GTT CCT TCC A-3'), a reverse primer (5'-ACT CTT TCC AGC CTT ACG CAA A-3') and a probe (5'-FAM-CAG AGC TGC AAA TGT C-3') derived from the YFV non-structural gene 3 (NS3) [10]. RT-qPCR was performed using the ABI 7500 Fast Real-Time PCR System (Applied Biosystems, Branchburg, NJ). For absolute quantification, standard curves were generated using five-fold dilutions of a cDNA plasmid template (plasmid pShuttle/YF17D) [11] of known concentration. On the basis of repeated standard curves, the lower limit of detection was established at 2111 copies/mg brain tissue, corresponding to a C_t value of 33. C_t values above 33 were considered below the limit of detection and represented as the square root of the lower limit of detection.

Correlation analysis

Correlation analysis was performed for data obtained from vaccine challenge experiments shown in Figure 3 (dose, IgG, nAbs, viral loads, and survival) and Figure S6 (dose, IgG, nAbs, and survival). Spearman correlation matrices were used to measure the strength of association among dose, IgG, nAbs, and viral loads.

Point biserial correlation was used to measure the association between survival and dose, IgG, nAbs, or viral loads. All calculations were done using GraphPad Prism Software (version 9) for calculation.

Statistical analysis

GraphPad Prism Software (version 9) was used for statistical analysis and statistical tests are indicated in each figure legend.

Results

YFV-specific humoral responses in different mouse models

In humans, YFV-specific humoral responses, especially nAbs are considered a correlate of protection against YFV infection [3]. To assess YFV-induced humoral responses in different mouse models, young adult (6–8 weeks of age) WT BALB/c and C57BL/6 mice were vaccinated with 2×10^4 PFU YF17D and treated with or without IFNAR-blocking antibody MAR1. Groups of *IFNAR*^{-/-} mice (on C57BL/6 background) were included as highly permissive positive controls.

In most untreated (i.e. no MAR1 administered) WT BALB/c (Figure 1(A) and S(2A)) and WT C57BL/6 mice (Figure 1(B) and S(2B)), YF17D vaccination induced no detectable or only very low levels of nAbs at day 7 or day 21 (Table S1A, limit of detection 1:20). However, high levels of YFV-specific IgG were elicited in both WT mice (with mean IgG titers $> 10^2$) and *IFNAR*^{-/-} mice (with mean IgG titers $> 10^5$) as early as 7 days post-vaccination and mounted to a plateau around 14 days post-vaccination (Figure 1(C,

D) and Figure S2 (C,D); Table S1B). Strikingly, MAR-1 treatment but not treatment with an isotype antibody control increased levels of IgG and nAbs in both WT mice by roughly one order of magnitude (Figure S1(A,B)). Nevertheless, the highest levels of antibodies were detected in *IFNAR*^{-/-} mice (Table S1), exceeding levels detected in both C57BL/6 and BALB/c mice, regardless of MAR1-treatment by up to 30- and 250-fold for nAb and IgG, respectively (Figure S2(A–D) and Table S1). Isotyping of IgG revealed an excess of IgG2a/c over IgG1, indicating that YF17D vaccination preferentially induced T-helper 1 (Th1)-biased antibody responses, consistently in all mouse models tested regardless of particular genetic background and presence of a functional type I IFN system. MAR1-treatment tended to enhance this Th1 polarization in both WT mice (Figure 1(E)).

YFV-specific cellular responses in different mouse models

In humans, YF17D vaccination induces vigorous CD4⁺ and CD8⁺ T cell responses, which leads to long-lived, polyfunctional T cell memory [6,7]. To characterize and compare YFV-specific T cell responses in different mouse models, we performed ELISPOT and flow cytometry with intracellular staining (ICS) of splenocytes four weeks after i.p. vaccination with 2×10^4 PFU of YF17D. Generally, C57BL/6 and BALB/c mice are well-known for their distinct polarization towards Th1 and Th2 immune responses, respectively, when encountered with the same antigen [41,42].

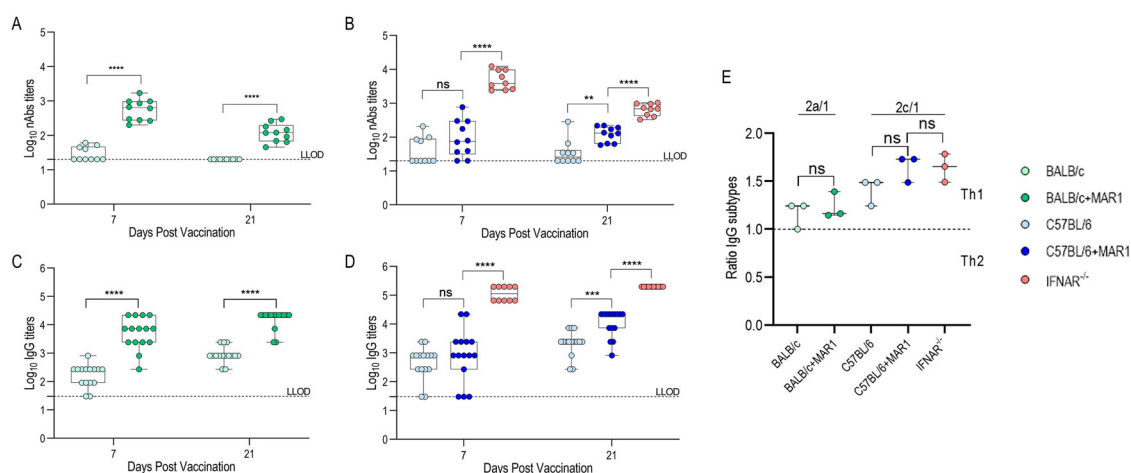


Figure 1. YFV-specific humoral responses in different mouse models. YFV-specific nAbs (A, B) and total IgG (C, D) levels at day 7 and 21 from mice vaccinated with 2×10^4 PFU of YF17D ($n \geq 9$ from two to three independent experiments). Boxes and horizontal bars denote the IQR and medians, respectively; whisker end points are equal to the maximum and minimum values. Statistical significance was determined using two-way ANOVA analysis between MAR1-treated and non-treated compartments (* $P < 0.05$; ** $P < 0.01$; *** $P < 0.001$; **** $P < 0.0001$, ns = not significant). Dotted lines denote the lower limit of detection (LLoD) of the assay. Ratio of IgG2a or IgG2c over IgG1 (determined for minipools of three mice each at day 28) plotted and compared to the original limit between Th1 and Th2 responses (E). Data are median \pm IQR. Statistical significance between groups was calculated by the nonparametric two-tailed Mann-Whitney *U*-test (ns = not significant, $P > 0.05$).

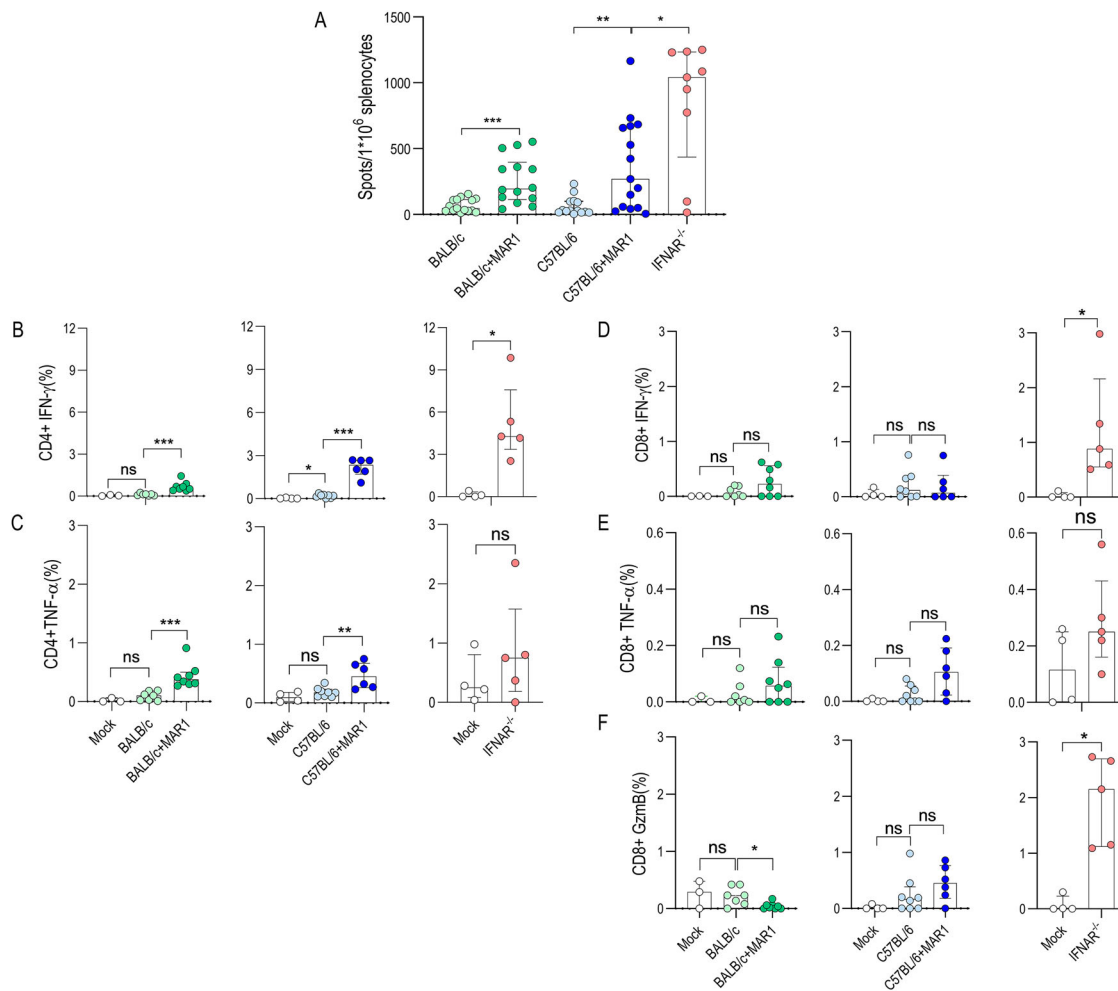


Figure 2. YFV-specific cellular responses in different mouse models. YFV-specific T cell responses were measured by IFN- γ ELISpot and flow cytometry with intracellular cytokine staining of splenocytes harvested from mice immunized with 2×10^4 PFU of YF17D at day 28 post-vaccination. (A) Spot counts for IFN- γ -producing cells per 10^6 splenocytes after 48 h stimulation with YF17D total antigen ($n \geq 9$ from two independent experiments). Percentage of IFN- γ (B), TNF- α (C) producing CD4 $^+$, and IFN- γ (D), TNF- α (E), GzmB (F) producing CD8 $^+$ T cells after overnight stimulation with YF17D total antigen ($n \geq 3$ from single experiment). All values normalized by subtracting spots/percentage of positive cells in corresponding unstimulated control samples. Data are median \pm IQR. Statistical significance between groups was calculated by the nonparametric two-tailed Mann-Whitney U -test (* $P < 0.05$; ** $P < 0.01$; *** $P < 0.001$; **** $P < 0.0001$, ns = not significant, $P > 0.05$).

In general, vaccination with YF17D elicited relatively weak T cell responses in untreated WT mice as confirmed by low numbers of IFN- γ producing splenocytes in ELISpot after stimulation with either YF17D total antigen (Figure 2(A)) or MHC-I restricted YFV peptides (Figure S3(A)) as recall antigens. This rather poor responsiveness was further confirmed by ICS showing a low percent of IFN- γ and TNF- α from CD4 $^+$ T cells after stimulation with YF17D total antigen (Figure 2(B,C)), and low expression of IFN- γ , TNF- α and GzmB from CD8 $^+$ after stimulation with either YF17D total antigen (Figure 2(D-F)) or MHC-I peptide (Figure S3(B-D)). Consistently, significantly more IFN- γ producing T cell and a higher percent of cytokine producing T cells were detected in all MAR1-treated WT mice; more pronounced in particular in C57BL/6 mice, as shown both in ELISpot (Table S2) as well as by ICS. Interestingly, MAR1-treatment promoted more

cells to produce Th1 cytokines in either WT mouse model after YF17D vaccination, including significantly more IFN- γ producing T cells (Figure 2(A) and Figure S3(A)) and substantially more IFN- γ and TNF- α expression CD4 $^+$ T cell (Figure 2(B,C)). Of note, MAR1-treatment had limited enhancing effects on CD8 $^+$ T cell responses in both WT mice, following recall with either YF17D total antigen (Figure 2(D-F)) or MHC-I peptide (Figure S3(B-D)). In line with antibody results, the highest number of IFN- γ producing T cells and the strongest cytokines production were detected in *IFNAR* $^{-/-}$ mice, exceeding that in either WT mice, regardless of MAR1-treatment (Table S2). Treatment with GIR isotype antibody had no significant effect on the IFN- γ produced from T cell in WT mice (Figure S1(C,D)). A pronounced expression of IL-2 (Th1-polarization), IL-4 (Th2-polarization), IL-17A (Th17), T-bet (Th1-polarization), or GATA3 (Th2-polarization) was not observed (not shown).

Protective efficacy of YF17D immunization against a lethal intracranial YFV challenge in different mouse models.

As a marked difference was seen in humoral and cellular responses in different mouse models, we wondered to what extent this may also translate into a distinct protective efficacy. To that end, mice were vaccinated with escalating doses of 2, 20 PFU, 2×10^3 PFU, 2×10^4 PFU of YF17D after they were treated, or left untreated, with MAR1. Three weeks later, they were intracranially challenged with 3×10^3 PFU of YF17D (Figure S5(A)). Intracranial (i.c.) challenge has been accepted as a stringent method for the evaluation of the protection conferred by YF17D and YF17D-derived vaccines in mice [43,44].

Consistently, both WT BALB/c and C57BL/6 vaccinated with escalating doses of YF17D produced considerable IgG (Figure 3(A,B) and Figure S6(A,B)) but barely detectable nAbs (Figure 3(C,D) and Figure

S6(C,D)) prior to challenge. However, intriguingly, a low dose of YF17D of as little as 2 and 20 PFU provided (almost) full protection in BALB/c (9/10 in 2 PFU group and 5/5 in 20 PFU group) (Figure 3(E) and Figure S6(H)), but failed to protect any C57BL/6 mice (0/10 in 2 PFU group and 0/5 in 20 PFU group) (Figure 3(F) and Figure S6(I)) from the same uniformly fatal i.c. challenge.

As expected, all mock-immunized mice experienced acute weight loss and progressed rapidly to severe neurological disease with ruffled fur, hunched posture and hind limb paralysis, and uniformly reached humane endpoints as early as 5 dpi for *IFNAR*^{-/-} and 8 dpi for WT BALB/c and C57BL/6 mice. While BALB/c mice vaccinated with either 2 PFU (Figure S5(F)) or 20 PFU (Figure S6(E)) survived with some weight loss, C57BL/6 mice suffered rapid weight loss and all mice had to be euthanized (Figure S5(G) and Figure S6(F)). These results suggested that

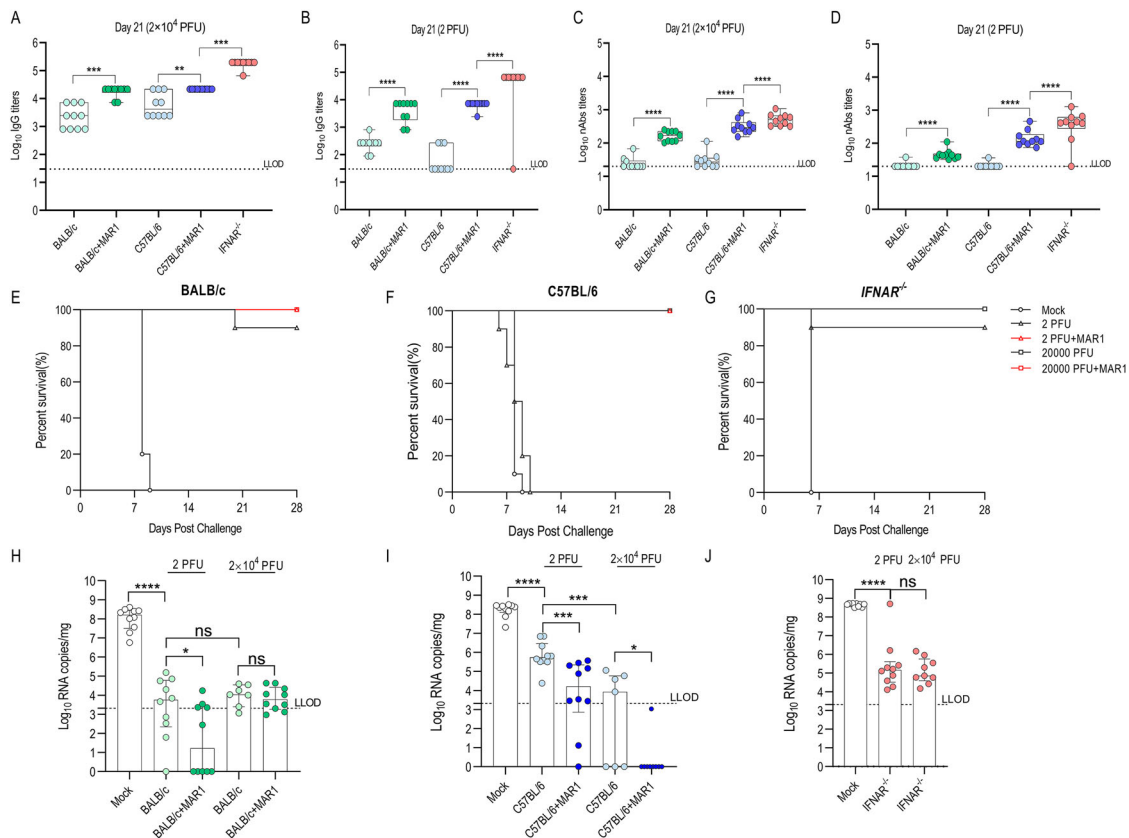


Figure 3. Mice were vaccinated with 2 PFU or 2×10^4 PFU of YF17D in presence or absence of MAR1 antibody, whereas *IFNAR*^{-/-} mice were vaccinated without MAR1-treatment. Mock group received culture medium alone ($n = 10$ from two independent experiments). Three weeks post-vaccination, animals were challenged i.c. with 3×10^3 PFU YF17D. **Pre-challenge YFV-specific IgG (A, B) and nAbs (C, D) levels in mice.** Boxes and horizontal bars denote the IQR and medians, respectively; whisker end points are equal to the maximum and minimum values. Statistical significance between groups was calculated by the nonparametric two-tailed Mann-Whitney *U*-test. (* $P < 0.05$; ** $P < 0.01$; *** $P < 0.001$; **** $P < 0.0001$, ns = not significant, $P > 0.05$). **Protective efficacy of YF17D against lethal intracranial challenge in different mouse modes.** Animals were monitored daily for survival for the next four weeks (E-F-G). Viral loads in the mouse brains at euthanasia. Brains were harvested from both sick mice at their euthanasia and mice that survived challenge until four weeks post-challenge ($n \geq 7$ from two independent experiments, mice died in four days post-challenge were excluded from experiments). RT-qPCR was performed on brain homogenates to determine viral RNA copies in the brain (H-I-J). Data are median \pm IQR. Statistical significance between groups was calculated by the nonparametric two-tailed Mann-Whitney *U*-test (* $P < 0.05$, ** $P < 0.01$, *** $P < 0.001$, **** $P < 0.0001$, ns = not significant, $P > 0.05$). Dotted lines denote the lower limit of detection (LLOD) of the assay.

YFV-specific IgG might be sufficient for YF17D-induced protection against intracranial challenge in WT mice, even without detectable nAbs. This was further supported by our observation that most BALB/c and C57BL/6 mice vaccinated with either 2×10^3 (Figure S6(A–D)) or 2×10^4 PFU (Figure 3(A,C)) of YF17D survived following i.c. challenge without producing any detectable nAbs, but only considerable IgG. Importantly, these data also demonstrate that YF17D-induced protection against i.c. challenge is strikingly mouse model dependent.

In *IFNAR*^{-/-} mice YF17D vaccination consistently elicited high levels of both IgG and nAbs, and provided full protection, regardless of initial inoculation dose. In the singular case (1/10) in which an *IFNAR*^{-/-} mouse that was immunized with 2 PFU (Figure 3(G)) was not protected, we noticed also no YF17D-specific IgG and nAbs (primary vaccination failure) (Figure 3(B,D)), supporting the key role of antibody response against YFV infection in immunocompromised *IFNAR*^{-/-} mice. In addition, all *IFNAR*^{-/-} mice (5/5) vaccinated with 2×10^4 PFU of UV-inactivated YF17D succumbed to challenge in the absence of any detectable IgG antibodies (Figure S7(A,B)). This demonstrates that active YF17D replication is critical for the induction of YFV-specific immunity and protection against YFV infection in immunocompromised *IFNAR*^{-/-} mice. Notably, generally post-challenge antibody levels were higher than pre-challenge antibody levels in all mouse models (Figure S5(B–E) and Figure S6(A–D)), which suggested that such single YF17D immunization could not induce sterilizing immunity in any mouse model.

We also compared viral loads in the mouse brains after i.c. challenge. In short, YF17D immunization massively restricted virus replication in the brain of all mouse models, even following vaccination with a minimal 2 PFU dose (Figure 3(H–J)). However, viral loads were detectable in the brains of most

YF17D-immunized mice that survived the challenge until four weeks post-challenge. This suggests that YF17D-specific immunity is unable to fully clear the YF17D virus from the mouse brains. All mock-immunized mice completely failed to control virus replication and presented with high viral loads in their brains (with mean RNA copies/mg $> 10^8$), with highest viral loads detected in the mock-immunized *IFNAR*^{-/-} group. Surprisingly, both 2 PFU and 2×10^4 PFU of YF17D vaccination showed an equally remarkable potency in restricting virus replication in the brains of WT BALB/c and *IFNAR*^{-/-} mice regardless of the vaccine dose (Figure 3(H,J)). By contrast in C57BL/6 mice, there was a clear dose-dependency and virus loads were around 100-fold lower in mice vaccinated with 2×10^4 PFU in comparison to mice vaccinated with 2 PFU (Figure 3(I)). These data demonstrate (i) the outstanding potency of YF17D-induced immunity in controlling YFV replication in the mouse brain, and (ii) mouse model-dependent sensitivity to i.c. challenge with YF17D. Moreover, there was a significant extra reduction of viral RNA copies in the brains of vaccinated WT mice with MAR1-treatment as compared to non-treated compartments (Figure 3(H,I)), except for BALB/c mice receiving a 2×10^4 PFU YF17D vaccination dose (Figure 3(H)).

Last, we performed a comprehensive correlation analysis to quantitatively define correlates of protection between pre-challenge humoral responses (nAbs and IgG levels) and the level of protection (survival and virus load) conferred by a wide range of YF17D doses in different mouse strains (Figure 4). Consistent with varying vaccine efficacy, also correlates of protection varied vastly among different mouse models. Firstly, in all models a clear correlation was observed between escalating vaccine doses used for immunization and an increase in IgG levels but, surprisingly, only a poor correlation with resulting nAbs levels

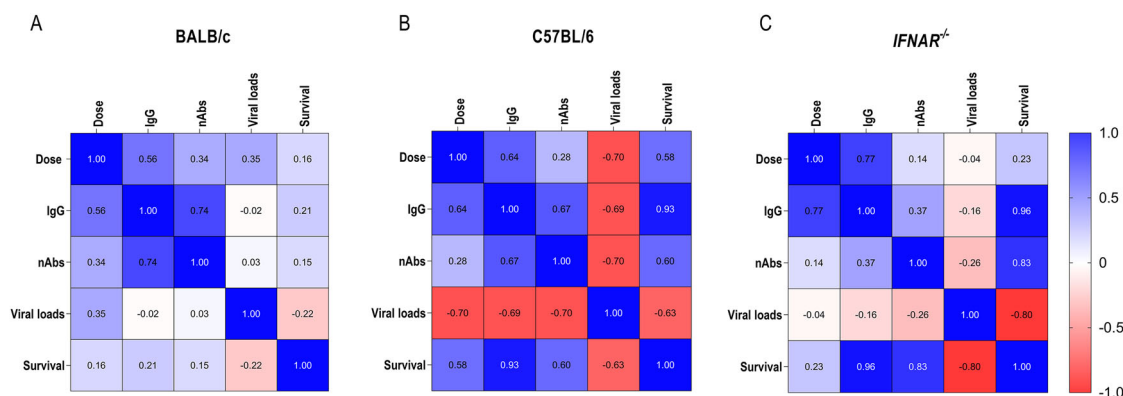


Figure 4. Correlation among vaccination dose (2 and 2×10^4 PFU), IgG, nAbs, viral loads, and survival in different mouse models. Correlation analysis was performed with data (dose, IgG, nAbs, viral loads, and survival), obtained from the experiment shown in Figure 3. Spearman correlation was used to measure the strength of association among dose, IgG, nAbs, and viral loads. Point biserial correlation was used to measure the association between survival and dose, IgG, nAbs, or viral loads. All coefficients are represented in the same heatmap (Correlation matrix and *P*-values were shown in Table S4A–S4B).

(Figure 4). In BALB/c mice, exclusively IgG levels strongly correlated with nAb levels (Figure 4(A); Table S4(A) and S4(B)). However, no further strong correlation was confirmed among other parameters in this model. In C57BL/6 mice, IgG levels showed a strong correlation with the YF17D dose used for vaccination, nAb levels and survival. Furthermore, viral loads in the brains after challenge inversely correlate with all other immune parameters and survival (Figure 4(B); Table S4(A) and S4(B)). In *IFNAR*^{-/-} mice which respond over the full range of escalating vaccine doses with uniformly high level of antibody levels and full survival, we also confirmed a poor correlation between vaccination doses with nAb levels, viral loads, and survival. Moreover, both IgG and nAb levels showed a strong correlation with survival but not viral loads after challenge, in line with the general importance of type I IFN signalling in controlling virus replication on one hand and failure to clear persistent virus replication from the brains of immunodeficient *IFNAR*^{-/-} mice (Figure 4(C); Table S4(A) and S4(B)).

Discussion

YF17D is one of the most efficacious human vaccines ever developed, and as such prototype of live-attenuated human vaccines in general [4]. Likewise, YF17D is employed as particularly potent viral vector for the development of novel vaccines [45]. However, molecular mechanisms of YF17D-induced protection are not fully understood, in part due to the absence of immunologically relevant immunocompetent small animal models [46]. Apart from non-human primates, hamsters represent the only immunocompetent model reproducing key symptoms of human yellow fever disease after infection with hamster-adapted YFV. However, due to the lack of reagents, YF17D-induced immune responses are difficult to address in the hamster model [14]. Likewise, despite limited mechanistic insight, nAb is widely accepted as immunological correlate of clinical protection [3]. Mouse models are most commonly used in preclinical vaccine research. Unfortunately, mice are resistant to YFV infection and show limited susceptibility for YF17D. Among many other factors hampering flavivirus infection [47,48], productive YF17D replication and hence vaccination is restricted by vigorous type I IFN responses in mice [21]. Therefore, also YF17D-derived vaccines are mainly assessed in immune-deficient mice missing key antiviral IFN- α / β receptors. However, while genetic ablation of IFN- α / β receptors in mice is associated with enhanced viral replication and thus vaccine potency, resulting immune responses might be skewed [32,33].

In humans, single-dose YF17D vaccination elicits a strong and long-lasting humoral response as assessed

in particular as YFV-specific nAb, which is considered a correlate of protection [3,5]. Here, both WT BALB/c and C57BL/6 mice responded to YF17D vaccination with limited nAb production. A significant increase in both nAbs and IgG could be elicited in WT mice after temporal blockade of IFN- α / β receptors, regardless of the dose inoculated (range 2–2 $\times 10^4$ PFU), alike in *IFNAR*^{-/-} mice. YF17D vaccination elicits broad and functional memory T cell responses in humans, which is an indispensable component of YF17D-induced protective immunity. YFV-specific CD4⁺ T cell responses represent a balanced Th1/Th2 phenotype, and CD8⁺ T cell responses are polyfunctional [6,7,49]. Similar to YF17D vaccination in *IFNAR*^{-/-} mice, temporal blockade of IFN- α / β receptors led to a remarkable increase in IFN- γ producing T cells (Figure 2(A) and Figure S3(A)), and stronger Th1-dominated cytokines production, including IFN- γ and TNF- α (Figure 2(B,C)) from CD4⁺ T cell in either MAR1-treated WT mice. However, slightly different from the human model in which T cell responses to YF17D tend to be more balanced and to contain a readily measurable Th2 component [50], YF17D vaccination in mice consistently resulted in largely Th1-dominated cytokines production and Th1-biased antibody responses in all five models tested, *IFNAR*^{-/-} and either WT mice regardless of MAR1-treatment. This is particularly remarkable considering that mice with a BALB/c background generally tend to mount Th2-dominated immune responses [41,42]. The significantly enhanced IFN- γ production from T cells, especially CD4⁺ T cells (Figure 2(B,C)), after temporal blockade of type I IFN signalling in turn may promote Th1 IgG class switching in either WT mice [51], matching with the relative increase in IgG2a/c isotype antibodies under latter condition (Figure 1(E)). Similar to findings from WNV-infected mice [52], the effect of MAR-1 on CD8⁺ T cells was less pronounced (Figure 2(D–F)). Nevertheless, our results are in line with the recently reported enhancement of CD8⁺ T cell responses and IgG production by temporal blockade of type I IFN signaling from YF17D, and other experimental vaccines based on unrelated live-attenuated RNA viruses, i.e. the vesicular stomatitis and lymphocytic choriomeningitis virus (LCMV) [34]. Additionally, our data highlight marked differences among mouse strains; as ablation of early-type I IFN signalling seems to have a stronger enhancing effects on T cell responses in WT C57BL/6 mice than in BALB/c mice.

YFV-specific nAbs are widely accepted as a major correlate of protection against YFV infection [3]. Interestingly, our data indicate that YFV-specific IgG may suffice, and nAbs levels might not be critical for vaccine-induced protection against lethal YF17D i.c. challenge in WT mice. Likewise, also humans may

remain protected after YF17D vaccination, despite not all subjects retain detectable nAbs [53], consistent with previous reports that, at least in mice, other immune compartments can provide protection against lethal viral infection even in the absence of nAbs or poor nAb responses [54,55]. Similarly, chimeric YF17D-derived vaccines against JEV or ZIKV that do not induce any YFV-specific nAbs in mice can fully protect against lethal YFV infection. In that case, protection to correlated with YFV-specific non-neutralizing antibodies and T cell responses targeting cell-associated YFV NS1 and other YFV non-structural (NS) proteins [37,56]. Thus, when novel YF17D-derived vaccines are being tested in mouse models, multiple parameters associated with vaccine efficacy and not just nAbs should be assessed.

Meanwhile, our results confirm the vital role of antibodies in YF17D-induced protection in immune-deficient *IFNAR*^{-/-} mice [20]. However, we demonstrate that *IFNAR*^{-/-} mice show an excessive susceptibility to YF17D vaccination with exceedingly high levels of IgG (Figure 3(A,B)) and nAb responses (Figure 3(C,D)), with no clear dose-dependency to escalating YF17D doses. In this context, immune-deficient *IFNAR*^{-/-} mice may not present an accurate mouse model for the evaluation of the immunity and protection conferred by YF17D (Figure 4(C)).

As challenge infection was performed intracranially, virus loads in the brain largely determined the fate of thus challenged mice, consistent with significantly higher viral RNA loads in the brains of mock-vaccinated animals (Figure 3(H-J)). YF17D vaccination dramatically restricted virus replication in the mouse brains in a strain and model-dependent manner. Surprisingly, even as little as 2 or 20 PFU of YF17D used for vaccination resulted in full control of virus replication in the brains of both WT BALB/c mice and immune-compromised *IFNAR*^{-/-} mice, yet not WT C57BL/6 mice. Intriguingly, either low dose (2 and 20 PFU) failed to elicit reasonable levels of YFV-specific nAbs in BALB/c and C57BL/6 mice. In this view, given i.c. challenge is commonly used to evaluate YF17D and YF17D-derived vaccine candidates in mice [37,43,44,56], extra caution should be taken when comparing results generated in different mouse models.

Type I IFN response plays a vital role in controlling flaviviruses infection, replication and dissemination, and in protecting the central nervous system (CNS) against flavivirus infection [21,57]. In line, much higher virus loads were detected in brains of mock-vaccinated *IFNAR*^{-/-} than WT mice (Figure 3(H-J)). Moreover, in particular, also CD8⁺ T cells were shown to be indispensable for long-term survival after intracranial YFV challenge, and infiltrations of YFV-specific CD8 T⁺ cells into the CNS improved virus control in mice [58]. Our data hence suggest

that even a minimal dose of YF17D may function as a trigger to protect the mouse CNS in a coordinated way with innate-type I IFN antiviral immunity.

In conclusion, we found that, even in the absence of detectable nAbs, YFV-specific IgG might be sufficient for YF17D-induced protection against intracranial challenge in WT mice. Second, the protective efficacy of YF17D is largely mouse strain-dependent, posing a dilemma for the choice of a preferred model. Multiple studies have demonstrated that YF17D induces balanced complex and polyvalent immune responses in humans. More than just humoral and cellular responses, various arms of innate and adaptive immunity conjointly contribute to the superior efficacy of YF17D [49,59]. Therefore, an animal model with an intact immune system should be more relevant to mimic YF17D immunization. We propose that C57BL/6 mouse with temporal blockade of IFN- α/β receptors during the early phase of immunization could serve as a complementary immunocompetent mouse model, which exhibits key features of YF17D-induced immunity, i.e. transient and self-limited replication of live-attenuated vaccine virus inducing nAb and Th1-polarized antiviral cellular immune responses in a dose-dependent manner. In contrast to more severely immune compromised type I and type II IFN receptor-deficient mice which YF17D vaccination leads to fatal neurotropic infection [19,37,56], YF17D is well tolerated in type I IFN receptor knockout mice and shows a very similar, yet quantitatively enlarged immune profile and may hence serve a convenient surrogate for the assessment of pre-clinical vaccine safety, immunogenicity and efficacy of YF17D and YF17D-based vaccines. Moreover, such modulation of innate antiviral signalling for the purpose of active YF17D vaccination in mice as validated in this study paves the way for advanced mechanistic studies, including in mice from different genetic backgrounds or transgenic lines available from the rich mouse genetic toolbox.

Acknowledgments

We thank Carolien De Keyzer and Lindsey Bervoets (Rega) for excellent technical assistance with animal experimentation as well as Katrien Geerts (Rega), Madina Rasulova and Jasmine Paulissen (TPVC-Rega) for help with serology assessment; likewise Geert Schoofs (Rega) for his assistance with flow cytometry set-up and instrumentation. We appreciate the continuing support from Dr Lotte Coelmont (Rega) for project management and her role in funding acquisition. The authors thank Dr Alan M. Watson, University of Pittsburgh for helpful discussion and suggestions regarding ICS gating strategies.

Disclosure statement

No potential conflict of interest was reported by the author(s).

Funding

This project has received funding from the European Union's Horizon 2020 research and innovation program [Grant Number 733176; RABYD-VAX consortium], and was supported by the Research Foundation Flanders (FWO) under the Excellence of Science (EOS) program [Grant Number 30981113; VirEOS project] as well as by the Belgian Science Policy Office (BELSPO) programme "Interuniversitaire attractiepolen" (IUAP) and the KU Leuven Rega Foundation. KD acknowledges grant support from KU Leuven Internal Funds [Grant Number C3/19/057; Lab of Excellence]. JM has received funding from the Chinese Scholarship Council (CSC) [Grant Number 201706760059].

ORCID

Ji Ma  <http://orcid.org/0000-0002-0912-2632>

Robbert Boudewijns  <http://orcid.org/0000-0002-5984-7279>

Lorena Sanchez-Felipe  <http://orcid.org/0000-0002-6928-0931>

Niraj Mishra  <http://orcid.org/0000-0002-8679-8847>

Thomas Vercruysse  <http://orcid.org/0000-0002-8649-777X>

Dieudonné Buh Kum  <http://orcid.org/0000-0001-8251-8230>

Hendrik Jan Thibaut  <http://orcid.org/0000-0001-5785-8276>

Johan Neyts  <http://orcid.org/0000-0002-0033-7514>

Kai Dallmeier  <http://orcid.org/0000-0002-8117-9166>

References

- Barrows NJ, Campos RK, Liao KC, et al. Biochemistry and molecular biology of flaviviruses. *Chem Rev.* 2018;118(8):4448–4482.
- WHO. Fact Sheet: Yellow fever. WHO Fact Sheet. 2019.
- Staples JE, Barrett ADT, Wilder-Smith A, et al. Review of data and knowledge gaps regarding yellow fever vaccine-induced immunity and duration of protection. *npj Vaccines.* 2020;5(1):1–7.
- Pulendran B, Oh JZ, Nakaya HI, et al. Immunity to viruses: Learning from successful human vaccines. *Immunol Rev.* 2013;255(1):243–255.
- Poland JD, Calisher CH, Monath TP, et al. Persistence of neutralizing antibody 30–35 years after immunization with 17D yellow fever vaccine. *Bull World Health Organ.* 1981;59(6):895–900.
- James EA, LaFond RE, Gates TJ, et al. Yellow fever vaccination elicits broad functional CD4+ T cell responses that recognize structural and nonstructural proteins. *J Virol.* 2013;87(23):12794–12804.
- Akondy RS, Monson ND, Miller JD, et al. The yellow fever virus vaccine induces a broad and polyfunctional human memory CD8+ T cell response. *J Immunol.* 2009;183(12):7919–7930.
- Bonaldo MC, Sequeira PC, Galler R. The yellow fever 17D virus as a platform for new live attenuated vaccines. *Hum Vaccines Immunother.* 2014;10(5):1256–1265.
- Boudewijns R, Ma J, Neyts J, et al. A novel therapeutic HBV vaccine candidate induces strong polyfunctional cytotoxic T cell responses in mice. *JHEP Reports.* 2021;3(4):100295.
- Sanchez-Felipe L, Vercruysse T, Sharma S, et al. A single-dose live-attenuated YF17D-vectored SARS-CoV-2 vaccine candidate. *Nature.* 2021;590(7845):320–325.
- Kum DB, Mishra N, Boudewijns R, et al. A yellow fever–Zika chimeric virus vaccine candidate protects against Zika infection and congenital malformations in mice. *npj Vaccines.* 2018;3(1):1–14.
- Pulendran B. Learning immunology from the yellow fever vaccine: Innate immunity to systems vaccinology. *Nat Rev Immunol.* 2009;9(10):741–747.
- Pulendran B. Systems vaccinology: probing humanity's diverse immune systems with vaccines. *Proc Natl Acad Sci USA.* 2014;111(34):12300–6.
- Julander JG. Animal models of yellow fever and their application in clinical research. *Curr Opin Virol.* 2016;18:64–69.
- Marin-Lopez A, Calvo-Pinilla E, Moreno S, et al. Modeling arboviral infection in mice lacking the interferon alpha/beta receptor. *Viruses.* 2019;11(1):35–25.
- Sarkar S, Heise MT. Mouse models as resources for studying infectious diseases. *Clin Ther.* 2019;41(10):1912–1922.
- Erickson AK, Pfeiffer JK. Spectrum of disease outcomes in mice infected with YFV-17D. *J Gen Virol.* 2015;96:1328–1339.
- Barrett ADT, Gould EA. Comparison of neurovirulence of different strains of yellow fever virus in mice. *J Gen Virol.* 1986;67(4):631–637.
- Meier KC, Gardner CL, Khoretonenko M V, et al. A mouse model for studying viscerotropic disease caused by yellow fever virus infection. *PLoS Pathog.* 2009;5(10):e1000614.
- Watson AM, Lam LKM, Klimstra WB, et al. The 17D-204 vaccine strain-induced protection against virulent yellow fever virus is mediated by humoral immunity and CD4+ but not CD8+ T cells. *PLoS Pathog.* 2016;12(7):e1005786–29.
- Erickson AK, Pfeiffer JK. Dynamic viral dissemination in mice infected with yellow fever virus strain 17D. *J Virol.* 2013;87(22):12392–7.
- Lobigs M, Müllbacher A, Wang Y, et al. Role of type I and type II interferon responses in recovery from infection with an encephalitic flavivirus. *J Gen Virol.* 2003;84(3):567–572.
- Bastard P, Michailidis E, Hoffmann HH, et al. Auto-antibodies to type I IFNs can underlie adverse reactions to yellow fever live attenuated vaccine. *J Exp Med.* 2021;218(4):e20202486.
- Hernandez N, Buccioli G, Moens L, et al. Inherited IFNAR1 deficiency in otherwise healthy patients with adverse reaction to measles and yellow fever live vaccines. *J Exp Med.* 2019;216(9):2057–2070.
- Fink K, Lang KS, Manjarrez-Orduno N, et al. Early type I interferon-mediated signals on B cells specifically enhance antiviral humoral responses. *Eur J Immunol.* 2006;36(8):2094–2105.
- Durbin JE, Fernandez-Sesma A, Lee C-K, et al. Type I IFN modulates Innate and specific antiviral immunity. *J Immunol.* 2000;164(8):4220–4228.
- Luft T, Pang KC, Thomas E, et al. Type I IFNs enhance the terminal differentiation of dendritic cells. *J Immunol.* 1998;161(4):1947–1953.
- Crouse J, Kalinke U, Oxenius A. Regulation of antiviral T cell responses by type I interferons. *Nat Rev Immunol.* 2015;15(4):231–242.

- [29] Le Bon A, Thompson C, Kamphuis E, et al. Cutting edge: enhancement of antibody responses through direct stimulation of B and T cells by type I IFN. *J Immunol.* 2006;176(4):2074–2078.
- [30] Thompson LJ, Kolumam GA, Thomas S, et al. Innate inflammatory signals induced by various pathogens differentially dictate the IFN-I dependence of CD8 T cells for clonal expansion and memory formation. *J Immunol.* 2006;177(3):1746–1754.
- [31] Kolumam GA, Thomas S, Thompson LJ, et al. Type I interferons act directly on CD8 T cells to allow clonal expansion and memory formation in response to viral infection. *J Exp Med.* 2005;202(5):637–650.
- [32] Clarke EC, Bradfute SB. The use of mice lacking type I or both type I and type II interferon responses in research on hemorrhagic fever viruses. Part 1: potential effects on adaptive immunity and response to vaccination. *Antiviral Res.* 2020;174:104703.
- [33] Zivcec M, Spiropoulou CF, Spengler JR. The use of mice lacking type I or both type I and type II interferon responses in research on hemorrhagic fever viruses. part 2: vaccine efficacy studies. *Antiviral Res.* 2020;174:104702.
- [34] Palacio N, Dangi T, Chung YR, et al. Early type I IFN blockade improves the efficacy of viral vaccines. *J Exp Med.* 2020;217(12):e20191220.
- [35] Lindenbach BD, Rice CM. trans-complementation of yellow fever virus NS1 reveals a role in early RNA replication. *J Virol.* 1997;71(12):9608–9617.
- [36] White JK, Gerdin AK, Karp NA, et al. XGenome-wide generation and systematic phenotyping of knockout mice reveals new roles for many genes. *Cell.* 2013;154(2):452–464.
- [37] Mishra N, Boudewijns R, Schmid MA, et al. A chimeric Japanese encephalitis vaccine protects against lethal yellow fever virus infection without inducing neutralizing antibodies. *MBio.* 2020;11(2):1–17.
- [38] Reed LJ, Muench H. A simple method of estimating fifty per cent endpoints. *Am J Epidemiol.* 1938;27(3):493–497.
- [39] Singh R, Rothman AL, Potts J, et al. Sequential immunization with heterologous chimeric flaviviruses induces broad-spectrum cross-reactive CD8+ T cell responses. *J Infect Dis.* 2010;202(2):223–233.
- [40] Maciel M, Kellathur SN, Chikhlikar P, et al. Comprehensive analysis of T cell epitope discovery strategies using 17DD yellow fever virus structural proteins and BALB/c (H2d) mice model. *Virology.* 2008;378(1):105–117.
- [41] Kuroda E, Kito T, Yamashita U. Reduced expression of STAT4 and IFN- γ in macrophages from BALB/c mice. *J Immunol.* 2002;168(11):5477–5482.
- [42] Watanabe H, Numata K, Ito T, et al. Innate immune response in Th1- and Th2-dominant mouse strains. *Shock.* 2004;22(5):460–466.
- [43] Putnak JR, Schlesinger JJ. Protection of mice against yellow fever virus encephalitis by immunization with a vaccinia virus recombinant encoding the yellow fever virus non-structural proteins, NS1, NS2a and NS2b. *J Gen Virol.* 1990;71(8):1697–1702.
- [44] Farm W, Station F, Albans S. Comparison of neurovirulence of different strains of yellow fever virus in mice. *J Gen Virol.* 1986;67:631–637.
- [45] Draper SJ, Heeney JL. Viruses as vaccine vectors for infectious diseases and cancer. *Nat Rev Microbiol.* 2010;8(1):62–73.
- [46] Douam F, Ploss A. Yellow fever virus: knowledge gaps impeding the fight against an old foe. *Trends Microbiol.* 2018;26(11):913–928.
- [47] Manet C, Roth C, Tawfik A, et al. Host genetic control of mosquito-borne Flavivirus infections. *Mamm Genome.* 2018;29(7):384–407.
- [48] Chen RE, Diamond MS. Dengue mouse models for evaluating pathogenesis and countermeasures. *Curr Opin Virol.* 2020;43:50–58.
- [49] Querec T, Bennouna S, Alkan S, et al. Yellow fever vaccine YF-17D activates multiple dendritic cell subsets via TLR2, 7, 8, and 9 to stimulate polyvalent immunity. *J Exp Med.* 2006;203(2):413–424.
- [50] Santos AP, Matos DCS, Bertho AL, et al. Detection of TH1/TH2 cytokine signatures in yellow fever 17DD first-time vaccinees through ELISpot assay. *Cytokine.* 2008;42(2):152–155.
- [51] Finkelman FD, Katona IM, Mosmann TR, et al. IFN-gamma regulates the isotypes of Ig secreted during in vivo humoral immune responses. *J Immunol.* 1988;140(4):1022–1027.
- [52] Pinto AK, Daffis S, Brien JD, et al. A temporal role of type I interferon signaling in CD8 + T cell maturation during acute West Nile virus infection. *PLoS Pathog.* 2011;7(12):e1002407–13.
- [53] Niedrig M, Lademann M, Emmerich P, et al. Assessment of IgG antibodies against yellow fever virus after vaccination with 17D by different assays: neutralization test, haemagglutination inhibition test, immunofluorescence assay and ELISA. *Trop Med Int Heal.* 1999;4(12):867–871.
- [54] Vogt MR, Dowd KA, Engle M, et al. Poorly neutralizing cross-reactive antibodies against the fusion loop of West Nile virus envelope protein protect in vivo via Fc receptor and complement-dependent effector mechanisms. *J Virol.* 2011;85(22):11567–11580.
- [55] Schmaljohn AL, Johnson ED, Dalrymple JM, et al. Non-neutralizing monoclonal antibodies can prevent lethal alphavirus encephalitis. *Nature.* 1982;297(5861):70–72.
- [56] Kum DB, Boudewijns R, Ma J, et al. A chimeric yellow fever-Zika virus vaccine candidate fully protects against yellow fever virus infection in mice. *Emerg Microbes Infect.* 2020;9(1):520–533.
- [57] Samuel MA, Diamond MS. Alpha/beta interferon protects against lethal West Nile Virus infection by restricting cellular tropism and enhancing neuronal survival. *J Virol.* 2005;79(21):13350–13361.
- [58] Bassi MR, Kongsgaard M, Steffensen MA, et al. CD8 + T cells complement antibodies in protecting against yellow fever virus. *J Immunol.* 2015;194(3):1141–1153.
- [59] Gaucher D, Therrien R, Kettaf N, et al. Yellow fever vaccine induces integrated multilineage and polyfunctional immune responses. *J Exp Med.* 2008;205(13):3119–3131.